Interplay of Spatial Reuse and SINR-determined Data Rates in CSMA/CA-based, Multi-hop, Multi-rate Wireless Networks

Ting-Yu Lin and Jennifer C. Hou
Department of Computer Science
University of Illinois at Urbana-Champaign

Abstract— In CSMA/CA-based, multi-hop, multi-rate wireless networks, spatial reuse can be increased by tuning the carrier-sensing threshold (T_{cs}) to reduce the carrier sense range (d_{cs}). While reducing d_{cs} enables more concurrent transmissions, the transmission quality suffers from the increased accumulative interference contributed by concurrent transmissions outside d_{cs}. As a result, the data rate at which the transmission can sustain may decrease. How to balance the interplay of spatial reuse and transmission quality (and hence the sustainable data rate) so as to achieve high network capacity is thus an important issue.

In this paper, we investigate this issue by extending Cali's model and devising an analytical model that characterizes the transmission activities as governed by IEEE 802.11 DCF in a single-channel, multi-rate, multi-hop wireless network. The systems throughput is derived as a function of T_{cs}, SINR, β, and other PHY/MAC systems parameters. We incorporate the effect of varying the degree of spatial reuse by tuning the T_{cs}. Based on the physical radio propagation model, we theoretically estimate the potential accumulated interference contributed by concurrent transmissions and the corresponding SINR. For a given SINR value, we then determine an appropriate data rate at which a transmission can sustain. To the best of our knowledge, this is perhaps the first effort that considers tuning of PHY characteristics (transmit power and data rates) and MAC parameters (contention backoff timer) jointly in an unified framework in order to optimize the overall network throughput. Analytical results indicate that the systems throughput is not a monotonically increasing/decreasing function of T_{cs}, but instead exhibits transitional points where several possible choices of T_{cs} can be made. In addition, the network capacity can be further improved by choosing the backoff timer values appropriately.

I. INTRODUCTION

With the increasing demands for a variety of bandwidth-hungry multimedia applications, the issue of how to push the wireless capacity to its possibly optimal limit has received much attention. Because the wireless medium is shared, media access control (MAC) protocol plays an important role of arbitrating medium access and optimizing the protocol capacity. In a CSMA/CA-based wireless network, such as the widely-deployed IEEE 802.11 standard, there are several component mechanisms that are related to medium access, collision resolution, and protocol capacity optimization: (i) *physical carrier sense* for detecting simultaneous transmissions and for mitigating interference; (ii) *binary exponential back-off mechanism* for resolving contention; and (iii) data rate adjustment according to the signal quality (such as the autorate function in IEEE 802.11).

physical carrier sense is a crucial mechanism for determining whether or not a node may access the medium. Before attempting for transmission, a node senses the medium and defers its transmission if the channel is sensed busy, i.e., the strength of the received signal exceeds a certain threshold T_{cs}. Physical carrier sense reduces the likelihood of collision by preventing nodes in the vicinity of each other from transmitting simultaneously, while allowing nodes that are separated by a safe margin (termed as the carrier sense range, d_{cs} to engage in concurrent transmissions. The second effect is referred to as *spatial reuse*. In spite of the simplicity, physical carrier sense has been shown in [9] to adversely limit the network capacity because of the inadequately chosen T_{cs}. Due to the signal capture effect, many would-be-successful transmissions are disabled by perhaps too conservative values of T_{cs}, limiting the effective spatial reuse in the network. While Jamieson *et al.* [9] suggest that physical carrier sense should be turned off to improve the throughput efficiency, we believe that *dynamically tuning T_{cs} according to the environmental changes would be more appropriate.*

After a node senses the medium to be idle, it engages in transmission. Whether or not the transmission succeeds then depends on the *Signal-to-Interference-and-Noise-Ratio* (SINR). If the SINR perceived at the receiver is smaller than a minimum SINR threshold β, the transmission cannot be correctly decoded and is thus failed. There are several causes for transmission failures. First, if nodes that are spatially close to each other *simultaneously* sense the medium to be idle and transmit, collisions occur. Second, the accumulative interference contributed by concurrent transmissions of multiple nodes outside d_{cs} could be so significant that it corrupts the transmission. The binary exponential back-off mechanism is designed to resolve contention and collision.

On the other hand, if the SINR perceived at the receiver exceeds β, the transmission is considered successful, but the data rate at which the transmission can sustain depends on the SINR value. Due to the significant advance in wireless modulation technologies, multiple *data transmission rates* are now available. For example, there are 4 data rates (1, 2, 5.5, 11 Mbps) available in 802.11b and 8 data rates (6, 9, 12, 18, 24, 36, 48, 54 Mbps) available in 802.11a/g. Usually the higher the SINR value, the higher the data rate at which the transmission can sustain. For a given value of SINR, one may then choose the highest possible data rate (that allows correct decoding for that given SINR value) in order to maximize systems throughput. Holland *et al.* [8] consider rate adjustment

based on the estimated channel quality at the receiver, and proposes a rate adaptive MAC protocol called the *Receiver-Based AutoRate (RBAR)* mechanism. As the name suggests, the intended receiver is responsible for evaluating the channel quality, and then reports this information back to the sender which then selects the highest possible data rate.

The value of SINR plays a vital role in determining whether or not a transmission is successful and/or the data rate the transmission sustain. It depends very much on how the value of T_{cs} is chosen. Conceptually a larger value of T_{cs} allows better spatial reuse, but the accumulative interference contributed by concurrent transmission outside d_{cs} may corrupt the transmission or deprive the transmission of sustaining a higher data rate. This represents a trade-off between spatial reuse and data rate selection, and suggests that *the operations of tuning T_{cs} and selecting data rates should be jointly considered in a unified framework.*

In this paper, we study the issue of balancing the interplay of *spatial reuse* (by tuning T_{cs}) and *data rate selection* (by selecting the highest possible data rate that can be sustained for a given SINR value), with the ultimate objective of maximizing the systems throughput. By extending Calí's model [6], we devise an analytical model that characterizes the transmission activities as governed by IEEE 802.11 DCF in a single-channel, multi-rate, multi-hop wireless network, and derive the protocol capacity as a function of T_{cs}, SINR, β, and other PHY/MAC systems parameters. We incorporate the effect of varying the degree of spatial reuse by tuning the T_{cs}. Based on the physical radio propagation model, we theoretically estimate the potential accumulated interference contributed by concurrent transmissions and the corresponding SINR. For a given SINR value, we then determine an appropriate data rate at which a transmission can sustain. While the carrier sense threshold and the transmit power are PHY-layer characteristics, the contention window size is a MAC-layer parameter. Unlike most previous studies, which only handle a single parameter at a time, we take a *cross-layer approach* and derive an analytical model that collectively considers PHY/MAC-layer parameters.

The theoretical analysis results show that the protocol capacity is not a monotonically increasing/decreasing function of T_{cs}. Instead, it exhibits transitional points where several possible choices of T_{cs} can be made. In addition, the protocol capacity can be further improved by choosing the backoff timer appropriately, although its effect is not as pronounced as that of tuning physical carrier sense.

The remainder of this paper is organized as follows. In Section II, we give an overview of existing work that aims to improve the systems throughput by tuning the carrier sense threshold or the transmit power in CSMA/CA wireless networks. In Section III, we give a succinct summary of IEEE DCF and the radio propagation model that characterize path loss, signal interference, and physical carrier sense. Following that, we present in Section IV the analytical model and report in Section V numerical results that give useful insights for improving the systems throughput. We validate the analytical model via simulation in Section VI. Finally, we conclude the paper in Section VII.

II. RELATED WORK

There are several *control knobs* that one can explore to control the degree of spatial reuse: the *transmit power* each node uses, the *carrier sense threshold* each node uses to determine if the shared medium is idle, and the *channel* on which a node transmits. The first two control knobs explore the *spatial diversity*, while the third control knob explores *channel diversity*. In this section, we give an overview of existing work that aims to improve network capacity by *spatial diversity*. While several researchers have explored use of channel diversity [4], [16], [3], we do not summarize these efforts, as they are remotely related to the problem considered in the paper.

A. Spatial Diversity by Tuning the Carrier-sensing Threshold

With the objective of increasing spatial reuse by tuning the carrier-sense threshold CS_{th}, several efforts have been made to either analytically or experimentally evaluate the effect of CS_{th} on the systems throughput performance [7], [17], [18], [19].

Guo *et al.* [7] investigate the spatial reuse issue in dense wireless ad hoc networks. The radio propagation and interference model is based on signal attenuation due to path loss (with path loss exponent γ) and SINR. They identify the minimum separation distance between two concurrent transmitters in chain and regular 2-D networks, so that the best achievable spatial reuse can be obtained. However, the MAC-layer overhead is ignored. Assuming a perfect MAC, Zhu *et al.* [19] propose an enhanced physical carrier-sensing mechanism using a similar methodology as [7]. Given the reception power, data rate, and network topology, they derive the value of CS_{th} that maximizes the systems throughput and achieves the best spatial diversity level in chain and 2-D grid networks.

Recently Zhai and Yang [18] present spatial reuse optimization mechanism by considering variable transmission distances, different receiver sensitivities, and multihop forwarding effects. They conclude that a single value of T_{cs} can be used for all the channel rates. In contrast, we assume the same receiver sensitivity and homogeneous transmission distance, and we have a different view of determining channel rates for different carrier sense ranges. Specifically, we scrutinize the best achievable data rate given a carrier-sensing setting. Different carrier sense thresholds render non-identical optimal data rates.

The work that comes closest to ours is perhaps that by Yang and Vaidya [17]. They indicate that the MAC overhead does have a significant impact on the choice of CS_{th}, and propose an analytical model to calculate the aggregate throughput in a wireless ad hoc network taking into account of the MAC overhead. They define two types of MAC overhead: bandwidth-independent (e.g., PLCP preamble and header, DIFS, SIFS) and bandwidth-dependent (e.g., channel- rate-dependent data frame time). Their results suggest use of a small carrier sense range to enable more concurrent transmissions. We share the same view. However, there are three major differences that differentiate our work from theirs. First, Yang and Vaidya [17] only consider the accumulative interference contributed by 1st-tier interference nodes. This has been shown to be inadequate in dense networks [7]. Our analytical model computes the accumulated interference contributed by all concurrent transmitters outside the carrier

sense range. Second, they do not associate data rates with carrier sense thresholds. In our work, we assign an appropriate data rate (a specific modulation scheme and coding rate) for each carrier-sensing threshold setting, based on the estimate of accumulative interference contributed by concurrent communications outside the carrier sense range. Third, they assume simultaneous transmissions within the carrier sense range always lead to collisions. Our analysis points out this may not be the case for a given data rate r_i, as long as the resulting accumulative interference does not exceed $P_r/\beta[i]$, where P_r is the received signal strength at the receiver, and $\beta[i]$ is the minimum SINR threshold for data rate r_i.

B. Spatial Diversity by Tuning the Transmit Power

Aiming at reducing interference and saving energy at power-constrained wireless/mobile devices, several topology control algorithms have been proposed for single-channel wireless networks [12], [13], [14]. Specifically, these algorithms determine (in a centralized or decentralized manner) the minimal transmit power with which each node should use, subject to network connectivity. Burkhart *et al.* [5], on the other hand, make a case that power control may not necessarily mitigate interference. They give a concise definition of interference, and show that most topology control algorithms do not necessarily help in interference reduction. Akella *et al.* [2] propose a power control and rate adaptation algorithm for a wireless LAN environment with tens of WiFi (IEEE 802.11) access points (APs) deployed in close proximity of each other. The main idea is to instrument APs to reduce their transmit power so that reasonable (even higher) system throughput may be sustained. Based on large-scale trace data from real-life networks, the authors in [2] conclude that by self-managing and self-adapting power and rate between APs, better network performance can be achieved.

In our analytical model, we assume a homogeneous transmit power at all nodes. Instead, we tune T_{cs}, and based on the resulting SINR value, determine an adequate data rate for each transmission. As indicated in [10], in the case that the achievable channel rate follows the Shannon capacity, spatial reuse depends only on the ratio of the transmit power to the carrier sense threshold. This implies tuning transmit power and T_{cs} has the same effect on spatial reuse.

III. NETWORK MODEL AND SIGNAL PROPAGATION/INTERFERENCE MODEL

In this section, we first give a succinct review of IEEE 802.11 MAC and several assumptions made, and then summarize the radio propagation model (that characterizes interference, path loss, and physical carrier sense).

A. Network Model

We consider a multi-hop, multi-rate wireless network that operates on IEEE 802.11 Distributed Coordination Function (DCF) [1]. Before a sender transmits, it performs physical carrier sense, and defers its transmission if the channel is sensed busy. If the channel is sensed idle for a specific time interval, known as the *Distributed Inter-Frame Spacing* (DIFS), the sender selects a backoff timer, uniformly distributed between [0,CW-1], where CW is the current *contention window size*. When the backoff
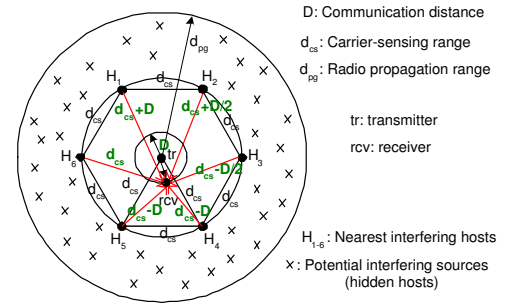

Fig. 1. An illustration that gives the definition of D, d_{cs}, d_{pg}, and 1st-tier interference nodes.

timer expires, the sender then attempt for transmission. If the submitted data frame is received correctly, the intended receiver sends an *acknowledge* frame (*ACK*) back to the sender after a specific time interval, known as the *Short Inter-Frame Spacing* (SIFS), which is shorter than DIFS. On the other hand, if the issued frame encounters collision or the ACK frame is not received, the data frame will be assumed to be lost. In this case, the sender schedules a re-transmission up to a pre-determined *retry* times, and doubles its contention window CW. The value of CW starts with CW_{min}, and doubles whenever unsuccessful transmission occurs until up to a pre-defined value of CW_{max}.

B. Radio Propagation and Interference Model

In this section, we describe the radio propagation and interference model that will be used in our analytical model. Fig. 1 gives an illustration of the various parameters that characterize radio propagation and interference. In real environments, the radio signal can be attenuated by several factors, including path loss (due to signal traveling over a distance), multi-path fading (due to signal reflections), and shadowing (due to obstacles in-between) [15]. In this paper, we only consider signal attenuation caused by path loss (with path loss exponent α). Specifically, let P denote the homogeneous transmit power of a sender, D the distance between the transmitter (tr) and the receiver (rcv), G the constant antenna gain, and α the path loss exponent (that typically ranges between 2 and 4), then the received power P_r can be expressed as $P_r = \frac{GP}{D^\alpha}$. We assume that the communication range D is short enough such that the receiver can sustain the highest data data with acceptable receiver sensitivity *without consideration of interference*.

As pointed out in [9], there exist several ways of implementing physical carrier sense in real devices. In this paper, we adopt the most commonly used approach: *energy detect*. That is, before a transmission attempt, the transmitter compares its currently sensed signal strength to T_{cs}. If the sensed signal strength exceeds T_{cs}, the channel is determined to be busy; and otherwise, idle. By $P_r = \frac{GP}{D^\alpha}$, we define the carrier sense range d_{cs} as

$$d_{cs} = \left(\frac{GP}{T_{cs}}\right)^{\frac{1}{\alpha}}. \tag{1}$$

Also, we define the radio propagation range d_{pg} as the maximum distance a wireless signal can reach under the signal attenuation specified in $P_r = \frac{GP}{D^\alpha}$.

When a transmitter tr transmits to a receiver, another *concurrent transmitter* may start to transmit if node tr is outside its

3

carrier sense range d_{cs}. By *concurrent transmission*, we refer to the transmissions that overlap in time at the receiver rcv. Whether the signal from node tr can be correctly decoded depends on the minimum SINR threshold. Specifically, we associate each data rate r_i with a minimum SINR threshold $\beta[i]$. The receiver rcv can correctly decode the signal at data rate $r[i]$ if the signal to interference power ratio (SINR) exceeds the corresponding SINR threshold $\beta[i]$, i.e., if

$$SINR = \frac{P/D^\alpha}{\sum_{t' \neq tr} P_{t'}/d(t',rcv)^\alpha} \geq \beta[i], \qquad (2)$$

then a data rate of $r[i]$ can be supported, where $d(t',rcv)$ is the distance between a concurrent transmitter t' and the receiver rcv.

In addition to the potential interference contributed by concurrent transmitters outside d_{cs}, there is another interference source — simultaneous transmissions, i.e., transmissions that start within a rather short period when the carrier is sensed. Interference contributed by simultaneous transmitters cannot be avoided by physical carrier sense and will induce collision.

Hexagon interference model:: The hexagon interference model has been used to to calculate the worst-case SINR given that every node senses the medium before attempting for transmission. Figure 1 shows the scenario in which the receiver rcv incurs the worst-case interference. By the definition of T_{cs}, the distance between any two adjacent concurrent transmissions is at least d_{cs}. H_1–H_6 constitute the six 1st tier interference nodes that are located at the closest possible locations to tr. It has been shown in [11] that the worst case interference (and hence the smallest SINR at receiver rcv) is incurred when rcv is so positioned that the six 1st tier interference nodes are, respectively, of distance $d_{cs} - D$, $d_{cs} - D$, $d_{cs} - D/2$, d_{cs}, $d_{cs} + D/2$, and $d_{cs} + D$ respectively. H_1-H_6 along with other transmitting nodes outside d_{cs} (within the propagation range d_{pg}) are potential interfering sources at the intended receiver rcv. Note that whether or not a transmission is successful and the data rate at which the transmission can sustain is dependent on the total interference level.

IV. Network Capacity as a Function of T_{cs}, SINR, and $\beta[i]$

In this section, we extend Calí's model to multi-hop, multi-rate wireless networks, and derive the network capacity as a function of d_{cs}, SINR, $\beta[i]$ and other PHY/MAC systems parameters. We first give a succinct summary of Calí's model, and discuss the various changes to be made to take into account of the effect of physical carrier sense, accumulative interference, and multi-data rate selection. Then we elaborate on our analytical model.

A. Calí's Model and Changes That Need to be Made

For analytical tractability, Calí *et al.* [6] consider a *p-persistent* version of IEEE 802.11 DCF, which differs from the standard protocol only in the selection of the backoff interval. Instead of using the binary exponential backoff timer values, the *p-persistent* version determines its backoff interval by sampling from a geometric distribution with parameter p. Due to the memoryless property of this geometric-distributed backoff
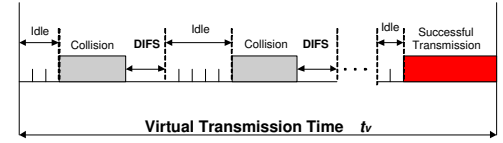

Fig. 2. Definition of the virtual transmission time in p-persistent IEEE 802.11 DCF protocol.

TABLE I

SYSTEMS PARAMETERS USED THROUGHOUT THE PAPER.

Parameter	Description
p_a	Probability that each node attempts for transmission when the medium is sensed idle
q	Parameter for the geometric distribution of the packet size, i.e., $\Pr\{packet\_length = i\ slot\} = q^{i-1}(1-q)$.
$\bar{m}$	Average transmission time, i.e., $\bar{m} = t_{slot}/(1-q)$
DIFS	Distributed interframe spacing
SIFS	Short interframe spacing
EIFS	Extended interframe spacing
ACK	Time required to transmit the ACK
$E(N_c)$	Average number of collisions in a virtual transmission time
$E(T_c)$	Average length of a collision period
$E(I)$	Average number of consecutive idle slots before a successful transmission or a collision
$E(S)$	Time required to complete a successful transmission (including all the protocol overheads), i.e., $E(S) = \bar{m} + SIFS + ACK + DIFS$.

algorithm, it is more tractable to analyze the *p-persistent* IEEE 802.11 protocol.

The analytic model is derived under the assumption that all the stations always have packets ready for transmission (which is termed the *asymptotic* condition [6]). Under the geometrically-distributed backoff assumption, the process that characterizes the occupancy behavior of the channel (idle slots, collisions, and successful transmission) till the end of each successful transmission is *regenerative*, with the sequence of time instants corresponding to the completion of successful transmission being the regenerative points. Calí *et al.* exploit this regenerative property and define the jth virtual transmission time as the time interval between the jth and $(j+1)$th successful transmissions. As shown in Figure 2, idle periods and collisions precede a successful transmission, where an idle period is a time interval in which the channel is idle due to the fact that all the back-logged stations are in the back-off mode, and a collision is the interval in which two or more stations attempt for transmission and their packets collide with one another.

Let t_v be defined as the average virtual transmission time, I_i and $T_{c,i}$ as the length of the ith idle period and the length of the ith collision in a virtual transmission time respectively. Given the major system parameters in Table I, the protocol capacity ρ can be expressed as $\rho = \frac{\bar{m}}{t_v}$, and we have

$$\begin{aligned} t_v &= E\left(\sum_{i=1}^{N_c}(DIFS + I_i + T_{c,i} + SIFS + ACK)\right) + E(I_{N_c+1}) \\ &\quad + E(S) \\ &= E(N_c) \cdot (E(T_c) + DIFS + SIFS + ACK) + (E(N_c) + 1) \cdot \\ &\quad E(I) + E(S), \qquad (3) \end{aligned}$$

where $SIFS$ and ACK in the first term on the right hand side of Eq.(3) is due to the extra waiting period in EIFS after

detection of an incorrectly-received frame (i.e., frame collision). Note that in Cali's model, it is assumed that each station waits for an interval of DIFS after a frame collision, while we assume the use of EIFS here.

The expressions of $E(N_c)$, $E(T_c)$, and $E(I)$ have been derived for single-cell WLANs:

$$E(N_c) = \frac{1 - (1 - p_a)^M}{M p_a (1 - p_a)^{M-1}} - 1, \tag{4}$$

$$E(T_c) = \frac{t_{slot}}{1 - (1 - p_a)^M - M p_a (1 - p_a)^{M-1}} \times$$
$$[\sum_{h=0}^{\infty} \{h \times [(1 - p_a q^h)^M - (1 - p_a q^{h-1})^M]\}$$
$$- \frac{M p_a (1 - p_a)^{M-1}}{1 - q}], \tag{5}$$

$$E(I) = \frac{(1 - p_a)^M}{1 - (1 - p_a)^M} \times t_{slot}. \tag{6}$$

Changes that have to be made:: To extend the p-persistent model to a multi-hop multi-rate wireless environment, we have to make several changes:

1) In the original p-persistent model, the attempt probability is solely determined by the backoff timer value. To incorporate the effect of physical carrier sense on the transmission opportunity, we re-define the *attempt probability* in our analytical model and figure in the carrier-sensing decision.

2) In the p-persistent model, collision is considered to occur if there is more than one simultaneous transmissions within a single cell. In our analytical model, we consider the effect of signal captures at different data rates (i.e., we define different minimum SINR thresholds to support different data rates), and define the notion of the *collision zone* (CZ). Essentially the collision zone is the area in which another single simultaneous transmission will impair the transmission of interest (and induce collision). All the nodes inside in the collision zone comprise *active nodes* as defined in [6]. Calculation of the collision probability is also modified accordingly.

3) In the p-persistent model, a single data rate is used for all transmissions. We incorporate multi-data rates (as afforded by the SINR) into our analytical model. A radio transceiver may have different signal capture capabilities based on the data rate (modulation and coding scheme) selected.

4) Because Cali's model is targeted at single-cell WLANs, they do not consider the issue of spatial reuse. In our analytical model, the degree of spatial reuse is controlled by tuning CS_{th} and impacts the number of concurrent transmissions that can take place (and hence the accumulative interference). The highest possible, sustainable data rate given the SINR can then be determined. Finally the network capacity is determined by the number of concurrent transmissions and the data rates they sustain.

To facilitate incorporation of the above changes in the analytical model, we make the following assumptions:

(A1) Nodes are distributed on a plane according to a Poisson point process with node density λ.

(A2) All the nodes always have packets ready for transmission, i.e., the *asymptotic* condition holds.

(A3) Every node uses the same power P and the radio propagation model given in Section III is used. For a transmission to be successful at data rate $r[i]$, the SINR at the receiver must exceed the minimum SINR threshold $\beta[i]$.

(A4) A sender and its corresponding receiver are close enough (as compared to d_{cs}) so that they share *approximately* the same view of simultaneous transmissions inside the collision zone and concurrent transmissions outside the carrier sense area.

B. Determination of Attempt Probability

Whether a transmission can take place or not depends on the *attempt probability*, p_a, of an intended transmitter. Recall that under the asymptotic condition, when a sender intends to transmit, it first senses the medium, and only if the wireless medium is sensed idle will the sender count down its backoff timer. The attempt probability is thus characterized by both physical carrier sense and binary exponential backoff. Specifically, in order for a transmission attempt to take place, the following independent events have to hold (from the system perspective): (i) E_1: No other nodes transmit within d_{cs}; (2) E_2: the accumulated interference, denoted as $I_{con,d_{cs},d_{pg}}$ and contributed by concurrent transmissions outside the carrier sense area, is below T_{cs}; and (3) E_3: the backoff timer of the sender counts down to zero. Consequently, p_a can be expressed as

$$p_a = \Pr\{E_1\} \times \Pr\{E_2\} \times \Pr\{E_3\}. \tag{7}$$

It is easy to see that $\Pr\{E_1\} = (1 - p_a)^{\lambda \cdot \pi d_{cs}^2}$. Also, $\Pr\{E_3\}$ is exactly the attempt probability derived in Cali's model, i.e., $b = \frac{2}{CW+1}$, where CW is the average contention window size.

To derive $\Pr\{E_2\} = \Pr\{I_{con,d_{cs},d_{pg}} \leq T_{cs}\}$, we need to derive $I_{con,d_{cs},d_{pg}}$. Let $K = \lfloor \frac{d_{pg} - d_{cs}}{d_{cs}} \rfloor + 1$. Let the ith-tier interference nodes of a sender are those at a distance of $i \cdot d_{cs}$ away from the sender. Under the hexagon interference model, there are approximately $\min(6i, \lambda \cdot (2\pi \cdot i \cdot d_{cs}^2))$ concurrent transmitters. Note that the first term considers the spatial reuse factor (i.e., two concurrent transmissions are separated by at least the distance of d_{cs}), while the second term denotes the average number of nodes in a ring with the inner radius $i \cdot d_{cs}$ and the outer radius $(i + 1) \cdot d_{cs}$. Thus we have

$$I_{con,d_{cs},d_{pg}} = \sum_{k=1}^{K} \frac{GP \min\{6k, 2k\lambda\pi d_{cs}^2\}}{(k d_{cs})^\alpha}. \tag{8}$$

Note that $I_{con,d_{cs},d_{pg}}$ is a function of d_{cs}. Given a fixed value of d_{cs}, $I_{con,d_{cs},d_{pg}}$ can be evaluated, and $\Pr\{E_2\}$ becomes an indicator function with binary values (0 or 1). If the value of d_{cs} is so chosen that $\Pr\{E_2\} = 0$, we consider those carrier sense configurations not desirable as they allow no transmission attempt.

Rates (Mbps)	$SINR$ Threshold β (dB)	Modulation	Coding Rate
54	24.56	64-QAM	3/4
48	24.05	64-QAM	2/3
36	18.80	16-QAM	3/4
24	17.04	16-QAM	1/2
18	10.79	QPSK	3/4
12	9.03	QPSK	1/2
9	7.78	BPSK	3/4
6	6.02	BPSK	1/2
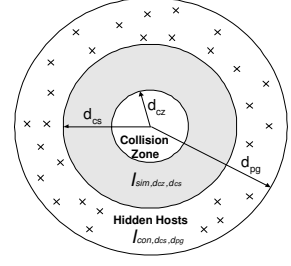
C. Determination of Sustainable Data Rates

Under assumption **(A4)**, the SINR perceived at the receiver can be approximately as

$$SINR = \frac{GPD^{-\alpha}}{I_{con,d_{cs},d_{pg}} + \eta} \qquad (9)$$

where η is the background noise in an additive white Gaussian noise (AWGN) wireless channel.

By Shannon's capacity theorem [15], the data rate R that can be achieved under the current carrier sense setting can be expressed as

$$R = W \log_2(1 + SINR), \qquad (10)$$

where W is the physical channel bandwidth in Hertz. On the other hand, the data rates supported in an IEEE 802.11-based network are discrete (with discrete SINR requirements). Table II gives the mapping of the minimum $SINR$ threshold $\beta[i]$ to the corresponding data rate $r[i]$ in the IEEE 802.11a standard [1]. If the $SINR$ calculated in Eq. (9) exceeds than the maximal value of β, 24.56, the data rate is set to 54 Mbps. On the other extreme, if the $SINR$ is smaller than the minimal value of β, 6.02, then the data rate supported is zero (no transmission). With discrete data rates and β values, we observe some *extra* interference level that an active communication can endure. Specifically, because of the difference between the SINR perceived at the receiver and the minimum SINR threshold $\beta[i]$ required to support a data rate $r[i]$, some extra interference contributed by *simultaneous* transmissions within the carrier sense area can be tolerated. We will elaborate on this in Section IV-D.

D. Definition of Collision Zone

As discussed in Section IV-C, to support a specific data rate $r[i]$, the SINR perceived at the receiver has to exceed $\beta[i]$. Because of the difference between the SINR perceived at the receiver and the minimum SINR threshold $\beta[i]$ required to support a data rate $r[i]$, some extra interference contributed by *simultaneous* transmissions within the carrier sense area can be tolerated. That means that *not* every single simultaneous transmission within d_{cs} will corrupt the transmission of interest. This also necessitates the definition of an area in which a single simultaneous transmission will impair the transmission of interest (and induce collision). All the nodes inside in this area are *active nodes* as defined in [6].

As illustrated in Fig. 3, we define the *collision zone* (CZ) as a circular area centered at the receiver with radius d_{cz} (whose

Fig. 3. Definition of *Collision Zone* (CZ).

value is yet to be determined). Any simultaneous transmissions inside CZ induce collision. Note that although physical carrier sense prevents *concurrent* transmissions inside d_{cs} from taking place, it cannot eliminate *simultaneous* transmissions inside d_{cs}. Therefore we need to estimate the accumulated interference contributed by simultaneous transmissions outside the CZ but within the carrier sense area, and see if this extra interference (in addition to $I_{con,d_{cs},d_{pg}}$) can be tolerated by $\beta[i]$. Let $I_{sim,d_{cz},d_{cs}}$ denote the accumulative interference contributed by simultaneous transmissions outside the CZ but inside the carrier sense area. It represents the *extra* interference level that should be tolerated in addition to $I_{con,d_{cs},d_{pg}}$ for a given data rate. To derive $I_{sim,d_{cz},d_{cs}}$, we divide the shaded area in Fig. 3 into K thin donuts, each with thickness of $\Delta d = (d_{cs} - d_{cz})/K$. For each thin donut, we calculate the interference contributed by senders in this area. By adding up all the interference, we can obtain $I_{sim,d_{cz},d_{cs}}$. Specifically,

$$
\begin{aligned}
&I_{sim,d_{cz},d_{cs}} \\
&\approx \sum_{k=1}^{K} \frac{PG}{(d_{cz}+d_k)^{\alpha}} \cdot p_a \cdot \lambda\pi[(d_{cz}+k\Delta d)^2 - (d_{cz}+(k-1)\Delta d)^2] \\
&= \lim_{K\to\infty} \sum_{k=1}^{K} \frac{p_a\lambda\pi P_{tx}G}{(d_{cz}+d_k)^{\alpha}} \cdot [(2k-1)\Delta d^2 + 2d_{cz}\Delta d] \\
&= \lim_{K\to\infty} \sum_{k=1}^{K} \frac{p_a\lambda\pi P_{tx}G}{(d_{cz}+d_k)^{\alpha}} \cdot [2(d_k - d_{cz} + \frac{\Delta d}{2})\Delta d - \Delta d^2 + 2d_{cz}\Delta d] \\
&= \lim_{K\to\infty} \sum_{k=1}^{K} \frac{p_a\lambda\pi P_{tx}G}{(d_{cz}+d_k)^{\alpha}} \cdot 2d_k\Delta d \\
&= 2p_a\lambda\pi P_{tx}G \int_0^{d_{cs}-d_{cz}} d \cdot (d_{cz}+d)^{-\alpha} dd. \qquad (11)
\end{aligned}
$$

Let $u = d_{cz} + d$. Thus $du = dd$ and $d = u - d_{cz}$. If $\alpha \neq 1$ and $\alpha \neq 2$, by substituting u for d, we have

$$
\begin{aligned}
&I_{sim,d_{cz},d_{cs}} \\
&= 2p_a\lambda\pi P_{tx}G \int_{d_{cz}}^{d_{cs}} (u-d_{cz})(d_{cz}+u-d_{cz})^{-\alpha} du \\
&= 2p_a\lambda\pi P_{tx}G \int_{d_{cz}}^{d_{cs}} (u^{1-\alpha} - d_{cz}u^{-\alpha}) du \qquad (12) \\
&= \frac{2p_a\lambda\pi P_{tx}G \left[(1-\alpha)d_{cs}^{2-\alpha} - (2-\alpha)d_{cz}d_{cs}^{1-\alpha} + d_{cz}^{2-\alpha}\right]}{(1-\alpha)(2-\alpha)}.
\end{aligned}
$$

Now to ensure that the transmission can sustain a data rate $r[i]$, all the accumulated interference outside the CZ plus the noise should not exceed the ratio of $P_r = P/D^{\alpha}$ and the SINR

6

threshold $\beta[i]$, i.e.,

$$I_{sim,d_{cz},d_{cs}} + I_{con,d_{cs},d_{pg}} + \eta \leq, \frac{P_{rcv}}{\beta} \qquad (13)$$

where $I_{con,d_{cs},d_{pg}}$ has been derived in Eq. (8). The radius d_{cz} can be obtained by computing the minimum value that satisfies

$$I_{sim,d_{cz},d_{cs}} \leq \frac{PGD^{-\alpha}}{\beta} - \eta - I_{con,d_{cs},d_{pg}}. \qquad (14)$$

Note that if the discrepancy between $\frac{GPD^{-\alpha}}{I_{con,d_{cs},d_{pg}}+\eta}$ and $\beta[i]$ is sufficiently large to accommodate extra interference contributed by simultaneous transmissions within d_{cs}, then d_{cz} will be small.

It is easy to see from the definition of the CZ, if any node inside the CZ transmits simultaneously with the transmission of interest, collision occurs. Hence, the number of active nodes, denoted by H, is the number of nodes inside CZ, i.e., $H = \lambda\pi d_{cz}^2$.

E. Calculation of Network Capacity

Recall that the virtual transmission time has been expressed as a function of $E(N_c)$, $E(T_c)$, $E(I)$, $E(S)$, and other MAC parameters (Eq. (3)). $E(N_c)$, $E(T_c)$, $E(I)$, and $E(S)$ have been in turn expressed as functions of the attempt probability p_a and the number of active stations H (Eqs. (4)–(6)). As we have derived both p_a and H for multi-hop, multi-rate wireless networks, we are in a position to derive $E(N_c)$, $E(T_c)$, $E(I)$, and $E(S)$.

First both $E(S)$ and $E(T_c)$ depend on the data rate at which the transmission or collision sustains. Let $\gamma = 1/r[i]$, where $r[i]$ is the data rate determined in Section IV-C. Then $E[S]$ can be expressed as

$$E[S] = \gamma \cdot \bar{m} + SIFS + \gamma \cdot ACK + DIFS, \qquad (15)$$

where both the data and acknowledgment frames are assumed to be sent at the specified data rate $r[i]$.

As indicated in [6], $E[T_c]$ is determined as the maximum frame length among all the colliding frames and has been expressed in Eq. (5). In addition to figuring in the data rate, the number of active nodes should be the number of nodes in the CZ. Thus $E(T_c)$ can be expressed in Eq. (16). Similarly, by "defining" the nodes in the CZ as the active nodes, we can express $E(N_c)$ as

$$E(N_c) = \frac{1 - (1-p_a)^H}{Hp_a(1-p_a)^{H-1}} - 1. \qquad (17)$$

To derive the expected idle period $E(I)$, we note that by physical carrier sense, whether or not a slot is determined to be idle depends on *all* the nodes within the carrier sense area. Hence, we have (assuming $M = \lambda\pi d_{cs}^2$)

$$E(I) = \frac{(1-p_a)^M \cdot t_{slot}}{1 - (1-p_a)^M} \qquad (18)$$

By plugging Eqs. (15)–(18) into Eq. (3), we obtain the virtual transmission time in multi-hop, multi-rate wireless networks. By $\rho = \frac{\bar{m}}{t_v}$, the protocol capacity in a carrier sense area can be obtained.

Derivation of network capacity: Now the network capacity C is the product of the total number of concurrent transmissions
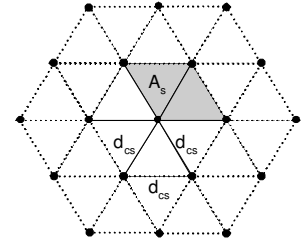

Fig. 4. Illustration of the consumed area $A_s = \frac{\sqrt{3}}{2} \cdot d_{cs}^2$ when there are infinite number of transmitters in the network.
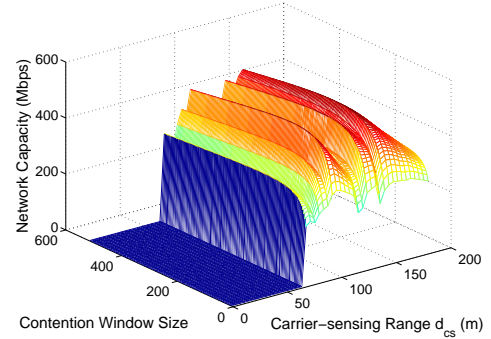

Fig. 5. Network capacity vs. T_{cs} and CW.

N_{tx} and the protocol capacity ρ in each carrier sense area. Let the total network area be denoted as A, and the "consumed area" by a transmitter as A_s. Obviously, $N_{tx} = \frac{A}{A_s}$. As depicted in Fig. 4, A_s ranges from $\frac{\sqrt{3}}{2}d_{cs}^2$ (in the case of a infinite number of transmitters) to $\frac{3\sqrt{3}}{2}d_{cs}^2$ (in the case of only one transmitter within the carrier-sensing area) [17]. To determine (approximately) the coefficient between the two extreme cases, we define a smoothing factor k and let $A_s = k \cdot \frac{\sqrt{3}}{2}d_{cs}^2$. If $\lambda\pi d_{cs}^2 \geq 7$, we consider there are an infinite number of transmitters and set $k = 1$. On the other hand, if $\lambda\pi d_{cs}^2 \leq 1$, we consider that the entire carrier sense area is consumed by a single transmitter and set $k = 3$. For other cases, we interpolate k between 1 and 3 based on the number of nodes inside d_{cs} (i.e., $\lambda\pi d_{cs}^2$) as follows:

$$\frac{7 - \lambda\pi d_{cs}^2}{\lambda\pi d_{cs}^2 - 1} = \frac{k-1}{3-k} \implies k = \frac{10 - \lambda\pi d_{cs}^2}{3}. \qquad (19)$$

V. NUMERICAL RESULTS

A. Joint Effect of T_{cs} and CW on Network Capacity

Fig. 5 illustrates network capacity vs. T_{cs} and CW. A total of 500 nodes are placed in a 500x500 square meters area ($\lambda = 0.002$), each with traffic load (1125 Bytes/packet). The distance between a sender/receiver pair is at most $D = 50$m. The parameter for the geometric distribution of the packet size is $q = 0.999$. The path loss exponent is $\alpha = 3$. The transmit power is set to $P = 0.012$mW resulting in a radio propagation range $d_{pg} = 650$m. As shown in the figure, while network capacity is affected by both d_{cs} and contention window size CW, it is more sensitive to d_{cs} (though CW still plays an important role under some scenarios to be shown below). Furthermore, network capacity is not a monotonically increasing/decreasing function of d_{cs} and CW. Instead, several transitional points exist. With standard arithmetical techniques, we obtain that the maximum

$$E(T_c) = \frac{\gamma \cdot t_{slot}}{1 - [(1-p_a)^H + Hp_a(1-p_a)^{H-1}]} \cdot [\sum_{h=1}^{\infty} h \cdot [(1-p_aq^h)^H - (1-p_aq^{h-1})^H] - \frac{Hp_a(1-p_a)^{H-1}}{1-q}] \tag{16}$$
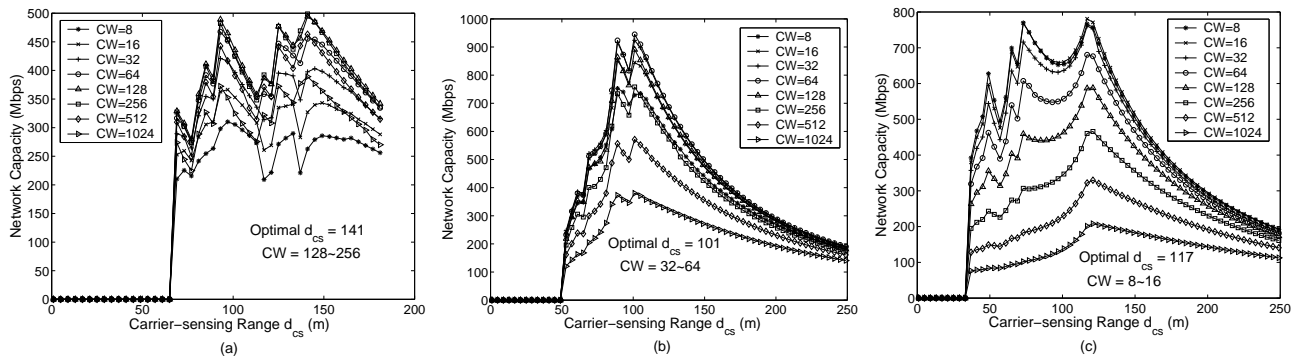

Fig. 6. Impact of node density on network capacity. (a) 500 nodes (extremely dense), (b) 250 nodes (dense), and (c) 125 nodes (moderately-populated) in a 500x500 m^2 area (with $\alpha = 3$ and packet size of 1125 Bytes).

network capacity is achieved when $d_{cs} = 141$ (or equivalently $T_{cs} = 4.28 \times 10^{-9}$mW) and $CW = 192$.

B. Impact of Node Density

Fig. 6 depicts the impact of node density on network capacity. While Fig. 6(a) has the same system parameters as Fig. 5, Fig. 6(b)–(c) change the node density to $\lambda = 0.001$ (250 nodes) and $\lambda = 0.0005$ (125 nodes), respectively.

In an extremely dense network (Fig. 6(a)), the network capacity is maximized when $d_{cs} = 141$ and $CW = 128 \sim 256$. Note that as discussed in Section V-A, network capacity is less sensitive to CW. This is corroborated by Fig. 6 (a). With $d_{cs} = 141$, the difference in network capacity by varying CW in the range of 128 and 256 is less than 0.1%. Another interesting finding in this extremely dense network is that, when d_{cs} grows beyond 180, T_{cs} becomes so small (physical carrier sense is so sensitive) that the value of indicator function $\Pr\{E_2\}$ in Eq. (7) always returns 0. Consequently, the attempt probability p_a remains zero, rendering a zero network throughput. On the other hand, when d_{cs} is smaller than 65, the accumulative interference always makes the SINR to fall below the minimum SINR threshold of 6.02. As a result, the data rate that can be sustained under such a d_{cs} setting (when $d_{cs} \leq 65$) is zero.

In addition to the optimal operational point at $d_{cs} = 141$, we observe another near-optimal operational point at $d_{cs} = 93$ and $CW = 128$. The difference in network capacity between the two operational points is less than 0.2%. For the optimal point with $d_{cs} = 141$, the maximum sustainable data rate is $r = 54$, while for the near-optimal point with $d_{cs} = 93$, the maximum sustainable data rate is $r = 18$. This suggests that network capacity can be maximized by assigning appropriate data rates to different carrier sense thresholds. The existence of several near-optimal operational points opens a new vista for localized adaptive algorithms.

Similar observations can be made in Fig. 6(b)–(c) as well. The network capacity first increases when the network changes from extremely dense (Fig. 6(a)) to dense (Fig. 6(b)), and then decreases from dense (Fig. 6(b)) to moderately-populated (Fig. 6(c)). Since different values of T_{cs} and CW are used for different node densities, this trend is caused by intricate interaction of spatial reuse and data rate selection. In general, as the number of nodes grows, network capacity increases (though not proportional to the node density) until the network becomes extremely dense (Fig. 6(a)), at which point network capacity degrades due to a large amount of medium contention activities. Another interesting finding is that d_{cs} decreases (except for a small increment from Fig. 6(b) to Fig. 6(c)) when the number of nodes decreases. Moreover, CW also decreases as the node density decreases. This suggests it is more desirable to increase T_{cs} and reduce CW to encourage more aggressive wireless channel access as the network becomes more sparse.

VI. VALIDATION OF ANALYTIC MODEL

TABLE III
PHYSICAL AND MAC PARAMETERS USED IN NS-2 SIMULATION.

Two-Ray Ground Propagation Model	
Slot time = 9 μs	(Omni-) Antenna Gain = 1
SIFS = 16 μs	Fixed Transmit Power P_{tx} = 0.012 mW
DIFS = 34 μs (2 Slot time + SIFS)	RXThresh = 1.02x10^{-10} mW
CW$_{min}$ = 8 CW$_{max}$ = 1024	Thermal Noise η = -95 dBm
Default CSThresh = 5.01x10^{-12} mW	

In this section, we conduct simulation to validate our analytical model, and compare the performance of analytical results with the optimal combination of (T_{cs}, CW, and r) and those with default values of T_{cs} and fixed data rates. The experiments are carried out based on the IEEE 802.11a standard. The mapping of data rates to their corresponding minimum SINR thresholds is shown in Table II. The simulation adopted is ns-2 with modifications on the interference model. Since original ns-2 processes only two signals at a time when determining if a frame is corrupted, the effect of accumulated interference in practical radio environments has been greatly ignored. Therefore we fix the ns-2 code to take accumulative interference into consideration. Whenever there is a new transmission activity,
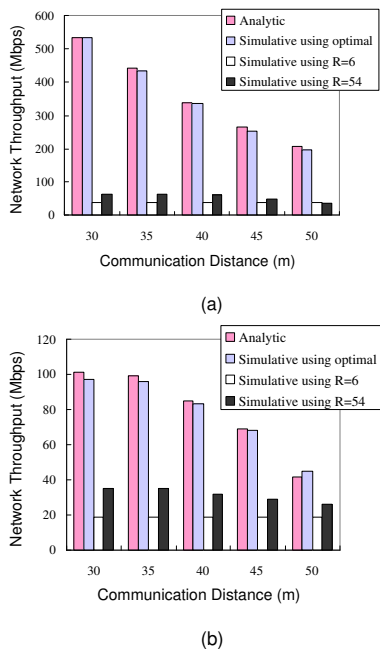
(a)

(b)

Fig. 7. Network capacity versus communication distance under different node densities: (a) 125 nodes and (b) 25 nodes in a 500x500 m^2 grid area (with the average packet size of 225 Bytes.

the extra interference contributed by the activity will be added up to re-evaluate whether or not the ongoing data transmission is corrupted. Only when the entire frame survives throughout the entire duration will the transmission be considered as successful. Table III summarizes the PHY and MAC parameters used in the simulation. RTS/CTS virtual carrier-sensing is disabled.

For the sake of comparison, we perform the experiments with three settings: (1) *simulation using optimal values* of T_{cs}, CW, and r; (2) *simulation using* $r = 6$; and (3) *simulation using* $r = 54$. The latter two settings use data rates of 6 and 54 Mbps with the default value of T_{cs} (Table III) and the exponential backoff window (CW_{min} and CW_{max} configured according to Table III). Fig. 7 depicts the network capacity versus the communication distance between the sender and the receiver with 125 (Fig. 7(a)) and 25 (Fig. 7(b)) nodes in a 500x500 grid network. Each sender generates single-hop CBR connections (with the average packet size of 225 Bytes) to saturate the network. The path loss exponent is set to $\alpha = 4$.

As shown in Fig. 7, the analytical results are quite consistent with simulation results with the optimal settings. This validates our analytical model. (We have other sets of simualtion results, but due to the page limit, do not show them in the paper.) On the other hand, simulative using $r = 6$ and $r = 54$ perform poorly partially due to the fact that the default value of T_{cs} is too sensitive, and the contention window size/data rate is not appropriately set.

VII. CONCLUSIONS

In this paper, we investigate the intricate interactions between several PHY- and MAC-layer parameters, including the carrier sense threshold T_{cs}, the contention window size CW, and the discrete data rates, in multi-hop, multi-rate wireless networks. By extending Cal$\acute{i}$'s model, we derive an analytic model that

characterizes the transmission activities as governed by IEEE 802.11 DCF in a single-channel, multi-rate, multi-hop wireless network. The network capacity is derived as a function of T_{cs}, SINR, β, and other PHY/MAC systems parameters. In particular, the effect of varying the degree of spatial reuse is incorporated by tuning the T_{cs}. Based on the physical radio propagation model, we theoretically estimate the potential accumulated interference contributed by concurrent transmissions and the corresponding SINR. For a given SINR value, we then determine an appropriate data rate at which a transmission can sustain. With the derived analytic model, one will be able to balance two contradicting factors: spatial reuse and sustainable data rates (determined as a result of the perceived SINR).

The theoretical analysis results show that the protocol capacity is not a monotonically increasing/decreasing function of T_{cs}. Instead, it exhibits transitional points where several possible choices of T_{cs} can be made. In addition, the protocol capacity can be further improved by choosing the backoff timer appropriately, although its effect is not as pronounced as that of tuning physical carrier sense.

REFERENCES

[1] IEEE 802.11a WG Part 11: Wireless LAN Medium Access Control (MAC) and Physical Layer (PHY) Specifications: High-speed Physical Layer in the 5 GHz Band. 1999.
[2] A. Akella, G. Judd, P. Steenkiste, and S. Seshan. Self Management in Chaotic Wireless Deployments. In *Proc. ACM MobiCom*, 2005.
[3] P. Bahl, A. Adya, J. Padhye, and A. Wolman. Reconsidering Wireless Systems with Multiple Radios. *ACM SIGCOMM Computer Communications Review (CCR)*, 34(5):39–46, Oct. 2004.
[4] P. Bahl, R. Chandra, and J. Dunagan. SSCH: Slotted Seeded Channel Hopping for Capacity Improvement in IEEE 802.11 Ad-Hoc Wireless Networks. In *Proc. ACM Int'l Conf. Mobile Computing and Networking (MobiCom)*, pages 216–230, 2004.
[5] M. Burkhart, P. von Rickenbach, R. Wattenhofer, and A. Zollinger. Does Topology Control Reduce Interference? In *Proc. ACM MobiHoc*, May 2004.
[6] F. Cali, M. Conti, and E. Gregori. Dynamic Tuning of the IEEE 802.11 Protocol to Achieve a Theoretical Throughput Limit. *IEEE/ACM Transactions on Networking*, 8(6):785–799, December 2000.
[7] X. Guo, S. Roy, and W. S. Conner. Spatial Reuse in Wireless Ad-hoc Networks. In *Proc. IEEE VTC*, 2003.
[8] G. Holland, N. Vaidya, and P. Bahl. A Rate-Adaptive MAC Protocol for Multi-Hop Wireless Networks. In *Proc. ACM/IEEE MobiCom*, July 2001.
[9] K. Jamieson, B. Hull, A. Miu, and H. Balakrishnan. Understanding the Real-World Performance of Carrier Sense. In *Proc. ACM SIGCOMM*, August 2005.
[10] T.-S. Kim, H. Lim, and J. C. Hou. Improving spatial reuse through tuning transmit power, carrier sense threshold, and data rate in multihop wireless networks. In *Proc. of ACM MobiCom*, September 2006.
[11] W. C. Y. Lee. Elements of Cellular Mobile Radio Systems. *IEEE Transactions on Vehicular Technology*.
[12] N. Li, J. C. Hou, and L. Sha. Design and Analysis of an MST-based Distributed Topology Control Algorithm for Wireless Ad-hoc Networks. *IEEE Trans. on Wireless Communications*, 4(3):1195–1207, May 2005.
[13] A. Muqattash and M. Krunz. A Single-channel Solution for Transmission Power Control in Wireless Ad Hoc Networks. In *Proc. ACM MobiHoc*, 2004.
[14] R. Ramanathan and R. Rosales-Hain. Topology Control of Multihop Wireless Networks Using Transmit Power Adjustment. In *Proc. IEEE INFOCOM*, March 2000.
[15] T. S. Rappaport. Wireless Communications: Principles and Practice (Second Edition). *Upper Saddle River Prentice-Hall*, 2002.
[16] J. So and N. Vaidya. Multi-Channel MAC for Ad Hoc Networks: Handling Multi-Channel Hidden Terminals Using A single Transceiver. In *Proc. ACM MobiHoc*, pages 222–233, May 2004.
[17] X. Yang and N. Vaidya. On Physical Carrier Sensing in Wireless Ad Hoc Networks. In *Proc. IEEE INFOCOM*, 2005.
[18] H. Zhai and Y. Fang. Physical Carrier Sensing and Spatial Reuse in Multirate and Multihop Wireless Ad Hoc Networks. In *Proc. IEEE INFOCOM*, April 2006.
[19] J. Zhu, X. Guo, L. L. Yang, and W. S. Conner. Leveraging Spatial Reuse in 802.11 Mesh Networks with Enhanced Physical Carrier Sensing. In *Proc. IEEE Int'l Conf. Communications (ICC)*, 2004.